Assessment and comparison of a recent kinematic sensitive subgrid length scale in Hybrid RANS-LES

A. Pont-Vílchez, F.X. Trias, A. Revell and A. Oliva

Abstract A recent kinematic sensitive subgrid length scale, Δ_{lsq}, initially developed for LES applications, is now considered for DES. Even though it is presented as a subgrid length scale, instead of a grey area mitigation (GAM) technique, this initial study shows how it could also be a good and natural approach for addressing this well-known DES shortcoming. In this paper, the Δ_{lsq} has been compared with a well-known kinematic sensitive length scale, $\tilde{\Delta}_{\omega}$. It includes a mesh resilience and a shear layer delay study with a Decaying Homogeneous Isotropic Turbulence configuration and two Backward Facing Step configurations, respectively. Encouraging results have been obtained, indicating Δ_{lsq} as a subgrid length scale to be considered.

1 Introduction

In the context of turbulence simulation approaches, the subgrid length scale, Δ, undoubtedly plays a crucial role in the approximation of the subgrid-scale viscosity, ν_{sgs} (Eq.1). However, in spite of this, it has not been given as much prominence as other parameters such as the model constant, C_m (C_{DES} in DES nomenclature), or the differential operator, $D_m(\bar{u})$.

$$\nu_{sgs} = (C_m \Delta)^2 D_m(\bar{u}) \tag{1}$$

A. Pont-Vílchez · F.X. Trias · A. Oliva
Heat and Mass Transfer Technological Center (CTTC)
Universitat Politècnica de Catalunya-BarcelonaTech (UPC)
ESEIAAT, Colom 11, E-08222 Terrassa, Barcelona, Spain.
e-mail: arnau@cttc.upc.edu
A. Revell
School of MACE, University of Manchester, UK.
e-mail: alistair.revell@manchester.ac.uk

Trias et al. [8] performed a comprehensive study of the spatial length scales used to date, concerned about the lack of consensus in the scientific community. Summarising the trends in modelling and simulation research, they identified that the volume cubic root, Δ_{vol} (Eq. 2), is used predominantly for LES applications, whereas the maximum length scale,$\Delta_{\max}$ (Eq. 3), is preferred for Hybrid ones. Mockett et al. [2] and Shur et al. [4] observed as both definitions were inextricably linked to unintended length scale changes due to mesh variations, as neither one considers the kinematic fluid behaviour; causing a poor mesh resilience for anisotropic meshes.

$$\Delta_{vol} = (\Delta x \Delta y \Delta z)^{1/3} \tag{2}$$

$$\Delta_{\max} = \max(\Delta x, \Delta y, \Delta z) \tag{3}$$

In this context, a kinematic sensitive approach resistant to mesh anisotropies was proposed by Mockett et al. [2], $\tilde{\Delta}_{\omega}$ (Eq. 4), defending the importance of using the maximum meaningful scale at each LES control volume. This method was improved by Shur et al. [4], Δ_{SLA} (Eq. 5), for $DDES/IDDES$ applications, where a rapid transition from RANS to LES is required to avoid unphysical instability delays.

$$\tilde{\Delta}_{\omega} = \frac{1}{\sqrt{3}} \max_{n,m=1,\dots,8} |l_n - l_m| \tag{4}$$

$$\Delta_{SLA} = \tilde{\Delta}_{\omega} F_{KH}(\langle VTM \rangle) \tag{5}$$

Where $l = \omega / \|\omega\| \times r_n$, r_n (n=1,...,8 for hexahedral cell) are the locations of the cell vertices and F_{KH} is a blending function which depends on the average *Vortex Tilting Measure* coefficient defined in Eq. 6.

$$VTM = \frac{|(S \cdot \omega) \times \omega|}{\omega^2 \sqrt{-Q_{\tilde{S}}}} \tag{6}$$

Where $\tilde{S}$ is the traceless part of the rate-of-strain tensor, $S = 1/2\left(\nabla \bar{u} + \nabla \bar{u}^T\right)$, i.e. $\tilde{S} = S - 1/3 tr(S) I$. Note that for incompressible flows $tr(S) = \nabla \cdot \bar{u} = 0$, therefore, $\tilde{S} = S$. Finally, Q_A refers to the second invariant of a second-order tensor A.

Although successful results have been obtained for a broad spectrum of fluid behaviours [2, 4, 1], a lack of physical meaning can be attributed to $\tilde{\Delta}_{\omega}$. In this regard, Trias et al. [8] suggested a new subgrid length scale only based on the velocity gradient, Δ_{lsq}. This subgrid length scale, which is derived from physical LES well-established assumptions, is not only resistant to grid anisotropies but also computationally inexpensive and adapted for any sort of grid, structured and unstructured ones.

$$\Delta_{lsq} = \sqrt{\frac{JG^TG : JG^TG}{G^TG : G^TG}}, J_i = \begin{pmatrix} \mathcal{J}_{ii}^x & & \\ & \mathcal{J}_{ii}^y & \\ & & \mathcal{J}_{ii}^z \end{pmatrix}, \mathcal{J}_{ii}^l = \frac{1}{\sum_{j!=i} \|G_{ij}^l\|} \quad (7)$$

Where J is the Jacobian, which colapses to $J = diag(\Delta x, \Delta y, \Delta z)$ in a Cartesian structured and non-uniform mesh. G_{ij}^l referes to the components of the gradient operator, G, in the l direction. It is important to note that the gradient tensor, G, is actually being computed in any LES and DES code. The Δ_{lsq} approach was tested in LES simulations (incompressible flow) using different kind of anisotropic meshes, showing good mesh resilience in all cases.

The rest of the paper is arranged as follows. In the next section, a brief description of the mathematical model is presented. In section 3, there is a detailed comparison of $\tilde{\Delta}_\omega$ and Δ_{lsq}, considering a simple (but meaningful) 2D case. In fact, this study was presented in Trias et al. [8], but this time the $\tilde{\Delta}_\omega$ performance is also examined. In section 4, the C_{DES} of a $DDES$ Spalart-Allmaras (SA) model is assessed with $\tilde{\Delta}_\omega$ and Δ_{lsq}, as well as their mesh resilience capabilities. Finally, subgrid length scales are tested in section 5 with two different Backward Facing Step configurations. These are: the experimental study of Vogel and Eaton [9] and the recent DNS of a BFS studied by Pont-Vílchez et al.[3]. The necessity of introducing a *Shear Layer Adaptative* technique into the Δ_{lsq} algorithm is also discussed.

2 Mathematical Model

The DDES turbulence model presented by Spalart et al.[6] has been used in this paper, including the Ψ term specially designed to override the unintended low-Re terms. All simulations carried out in this study have been run using *OpenFOAM* . The hybrid convection scheme presented by Travin et al. [5] for hybrid $RANS/LES$ calculations is used. For the temporal discretisation, a 2^{nd}-order implicit backward scheme is considered. The velocity-pressure system is coupled using the well-known $PISO$ algorithm. Concerning the boundary conditions, they can be found in the respective references.

3 Comparison of subgrid length scales for a 2D simplified flow

First, the $\tilde{\Delta}_\omega$ and Δ_{lsq} performance is assessed in 2D simplified flow, based on the following parameters,

$$\Delta = \begin{pmatrix} \beta & \\ & \beta^{-1} \end{pmatrix}, G = \begin{pmatrix} 0 & 1 \\ 1-2\omega & 0 \end{pmatrix} \tag{8}$$

which is displayed in Figure 1. Notice that the size of the control volume remains equal to unity; therefore, $\Delta_{vol} = 1$, regardless of the value of β. Even though turbulence is a clearly 3D phenomenon, this analysis in 2D helps to understand the most essential properties of each length scale. For instance, in a 2D motion $\tilde{\Delta}_\omega = \sqrt{(\beta^2 + \beta^{-2})/3}$ only depends on the β ratio, but is not sensitive neither the flow behaviour nor the volume rotation (the same results is obtained with $\beta = 5$ and $\beta = 1/5$). In contrast, Δ_{lsq} is adapted depending on the flow behaviour and the cell orientation, providing completely different values in the simple shear ($\omega = 0.5$) case. In that situation, the spatial length scale is reduced to $\beta^{-1} = \Delta y$, completely depending then on the wall mesh refinement. This capability propitiates the physical instabilities in Grey Area regions, as in those situations the flow normally exhibits a *2D-like simple shear* and is also accompanied by strong mesh refinements (close to the wall). In the other hand, this severe reduction could sadly damage the LES/RANS domain, which is defined by the $\tilde{d}$ coefficient. The original DES [7] would be highly influenced by the new Δ_{lsq}, but it seems as it is not the case for the Delayed DES [6], which present a good resilience to the different Δ behaviours (see section 5). However, a rigorous study should be carried out in this area, as it could affect other flow configuration not treated so far.

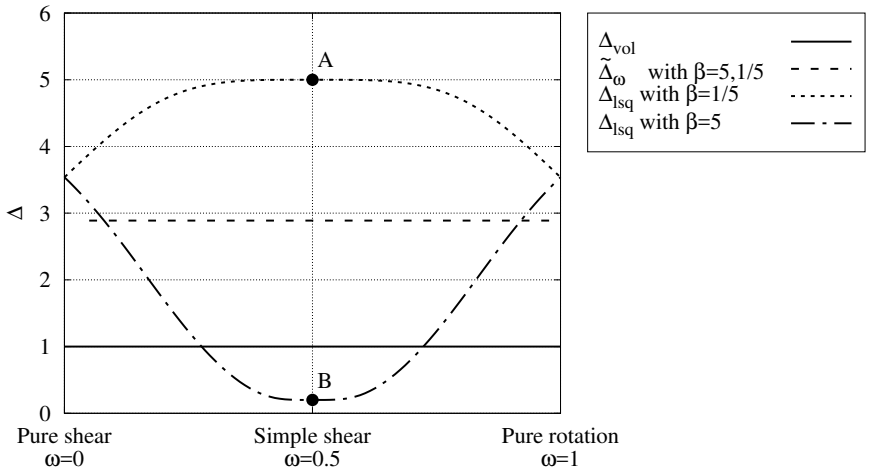

Fig. 1 Comparison between $\tilde{\Delta}_\omega$ and Δ_{lsq} for the simple 2D flow defined in Eq. 8 with different values of $\beta = 1/5, 1/2, 2, 5, 10$

4 Decaying Homogeneous Isotropic Turbulence (DHIT)

The subgrid length scale properties mentioned in the previous section have been tested in a DHIT case (Wray [10] configuration), where the DDES turbulence model acts in LES mode. Different C_{DES} coefficients have been analysed, concluding that $C_{DES} = 0.65$ is the most appropriate, regardless of the subgrid length scale. The study considering different C_{DES} has not been included in this work, but it is worth noting that both meshes, 32^3 and 64^3 have been studied. Regarding the subgrid length scale resilience in anisotropic meshes, a couple of cell configurations have been considered in figure 2, *Book* ($32 \times 32 \times N$,left) and *Pencil* ($32 \times N \times N$,right), respectively. First, $\Delta_{\max}$ is too dissipative with anisotropic meshes in both situations, but

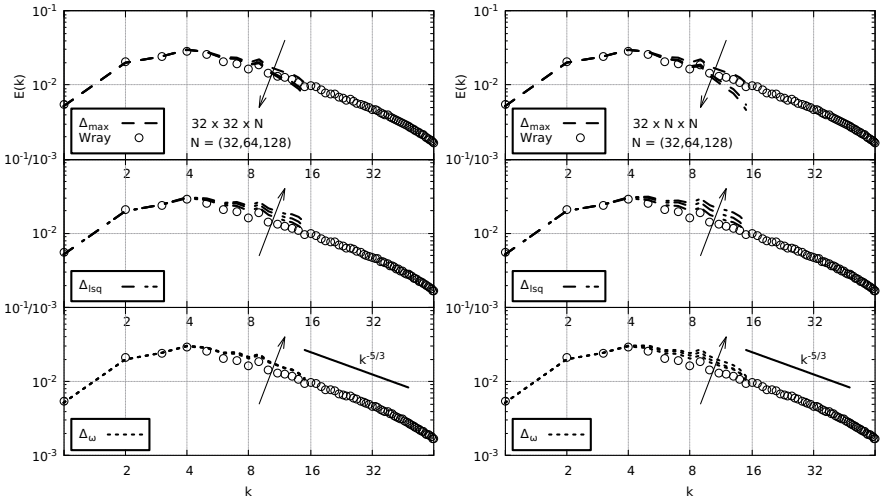

Fig. 2 Assessment of the mesh resilience capabilities for different subgrid length scales in a DHIT ($C_{DES} = 0.65$) case; $\Delta_{\max}$ (top), Δ_{lsq} (middle) and $\tilde{\Delta}_{\omega}$ (bottom). "*Book*" (left) and "*Pencil*" (right) cells are considered.

their effects are pronounced in the *Pencil* case, where the length scale clearly underestimate the mesh capabilities for solving turbulence. The contrary is true in the Δ_{lsq} case, where the dissipation introduced by the DDES model is not enough, increasing the energy retained in the smallest scales. This behaviour can be attributed to the subgrid length scale property discussed in section 3, where Δ_{lsq} allows values similar to the smallest scale (β^{-1}). However, in contrast to $\Delta_{\max}$, the same reaction is observed for *Book* and *Pencil* cells, indicating a beneficial lack of sensitivity to the kind of mesh anisotropy. Finally, the most robust behaviour is presented by $\tilde{\Delta}_{\omega}$, which is not influenced at all in the *Book* shape and only small discrepancies are observed in the *Pencil* case. This feature is associated with the intrinsic defi-

nition of the subgrid length scale, where the diagonal value of the cell volume is assessed. By definition, it means that $\tilde{\Delta}_\omega$ is always going to depend at least on 2 dimensions, being sensitive to the mesh anisotropies, but at the same time limiting their downward excursions, something that cannot be guaranteed in the Δ_{lsq}.

5 Results and Discusions

Once the properties of the subgrid length scale have been assessed in a fully 3D turbulent case (DHIT), their influence on switching from RANS to LES is analysed in two BFS configurations. BFS is a well-known studied case in Hybrid turbulence modelling, where the flow separation is induced by the geometry and the resulting shear layer downstream of the step-edge is delayed because of the undesired smooth RANS-LES transition (Grey Area). The first BFS resembles the experimental study carried out by Vogel and Eaton [9] at $Re_h = 28000$ and expansion ratio (ER) equal to 5/4, where Re_h is based on the step height and the inflow bulk velocity U_b. In contrast, the other BFS is a DNS carried out by Pont-Vilchez, A. et al [3] at $Re_h \sim 13700$ and $ER = 2$, which provides high-quality data for assessing the forecasting capabilities of existing/new turbulence models subjected to sudden expansions. The Re_τ at the inflow of each BFS are 2500 and 395, which hereafter are named *BFS-VE* and *BFS-DNS* , respectively. The influence of the unsteady flow (LES area) into the RANS zone is perceived in the *BFS-DNS* , whereas it is negligible in the *BFS-VE* due to the LES zone remains far from the upper wall region. Apart from that, the Re_h value of the *BFS-VE* is significantly higher than the *BFS-DNS* , studying then the subgrid length scale performance at high and moderate Re values. Therefore, the reasons for selecting two different BFS geometries are clear. Both configuration share the same coordinate system, which is located at the step edge.

5.1 BFS-VE ($Re_h = 28000, ER = 5/4$)

A boddy fitted mesh with $300 \times 78 \times 60$ grid points has been used to cover the computational domain in the stream-wise (x_1), normal (x_2) and span-wise (x_3) directions, respectively. The same boundary conditions used by Spalart et al. [6] have been considered. First, the differences observed between Δ_{lsq} and $\tilde{\Delta}_\omega$, as well as the improvements provided by the Δ_{lsq}, can be explained/summarised using Fig. 3 and Fig.1. Fig. 3 shows the evolution of various Δ along the stream-wise direction and a detailed view (zoom) at the shear layer zone. $\Delta_{\max}$ exhibits the highest values, providing too much dissipation into the shear layer and contributing to an excessive delay. An

important reduction of Δ values is presented by $\tilde{\Delta}_\omega$, as the flow detect a 2D flow behaviour in the x_1x_2 plane downstream of the step edge (Grey Area), ignoring the Δx_3 and collapsing to the diagonal value in that plane, $\tilde{\Delta}_{\omega-2D} = \sqrt{\Delta x_1^2 + \Delta x_2^2/3}$. Even though this is the initial behaviour (Fig.3, right), turbulence is triggered in the shear layer (around 1-2h) switching from $2D$ to $3D$ ($\tilde{\Delta}_{\omega-3D}$). It is worth noting here that $\tilde{\Delta}_\omega$ will never provide values lower than the lowest cell volume $2D$ diagonal (Eq.9). Where coefficient 3 was artificially introduced for recovering $\Delta_{\max}$ behaviour in the DHIT case with cubic cells.

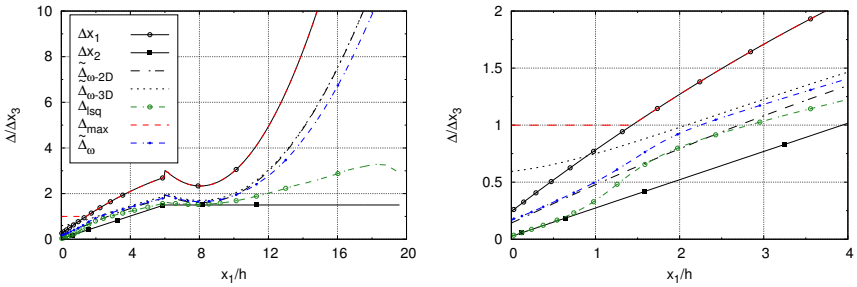

Fig. 3 Average of the subgrid length scales from the step edge to the outflow (left) and a zoom view downstream of the step edge (right). Where $\tilde{\Delta}_{\omega-2D} = \sqrt{\Delta x_1^2 + \Delta x_2^2/3}$ and $\tilde{\Delta}_{\omega-3D} = \sqrt{\Delta x_1^2 + \Delta x_2^2 + \Delta x_3^2/3}$ refer to the vortex located in the x_1x_2 plane (KHinstabilities) and 3D Homogeneous Isotropic Turbulence, respectively.

$$\tilde{\Delta}_{\omega\min} = \min_{i!=j} \left(\sqrt{\Delta x_i^2 + \Delta x_j^2/3} \right) \tag{9}$$

In contrast, Δ_{lsq} can provide values as lower as the wall mesh refinement allows Δx_2 (the order of wall units in RANS-LES simulations), as has been demonstrated and discussed in Section 3 for simple shear dynamics. This is exactly the case of the BFS (and many others), where a strong reduction of Δ values can be observed (in comparison to $\tilde{\Delta}_\omega$) significantly diminishing the eddy viscosity and unlocking the KHinstabilities. Once the $KH$are triggered (0.5-1.5h), Δ_{lsq} switches its behaviour to a diagonal-trend similar to $\tilde{\Delta}_{\omega-2D}$. It corresponds to the "Pure rotation" mentioned in Fig.1.

The reduction of the shear layer delay can be perceived in Fig.4, comparing the rms values along the stream-wise direction using Δ_{lsq} and $\tilde{\Delta}_\omega$. Apart from observing how both Δ provide good results at $x_1 = 3.2h$ (left), and a clear improvement of Δ_{lsq} in comparison to $\tilde{\Delta}_\omega$ from $0h$ to $2h$ (right), Fig.4 also shows how both Δ unlock KH instabilities from the step-edge ($x_1 = 0$). This is not the case for other spatial length scales, which do not depend on the flow kinematics. Finally, the skin friction,$\langle C_f \rangle$, at the lower and upper walls are shown in Fig. 5, presenting a good agreement with the reference data obtained by Shur et al. [4]. In that case, the differences between both subgrid

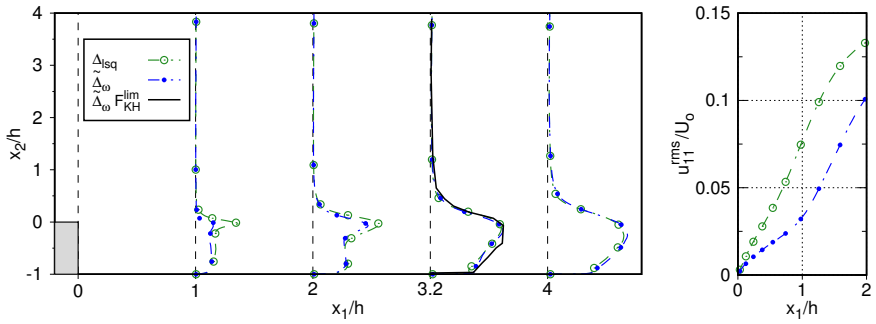

Fig. 4 Resolved Reynolds stresses in the stream-wise direction (u_{11}^{rms}) considering various subgrid length scales (left) and its evolution at $x_2 = 0$ (right). Where U_o refers to the inflow bulk velocity. Reference data, $\tilde{\Delta}_\omega F_{KH}^{lim}$, has been obtained from Shur et al. [4].

length scales is minimum, observing only small discrepancies in favour of the Δ_{lsq}, close to the outflow.

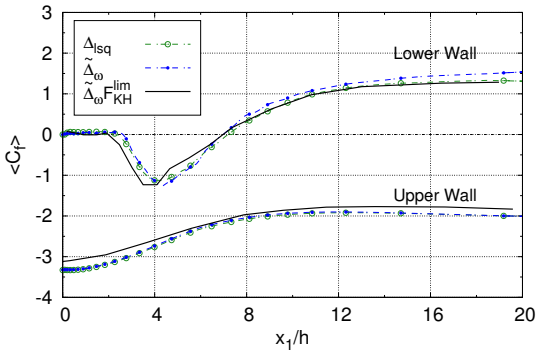

Fig. 5 Skin friction, $\langle C_f \rangle$, at the lower and upper walls downstream of the step edge. Reference data, $\tilde{\Delta}_\omega F_{KH}^{lim}$, has been obtained from Shur et al. [4].

5.2 BFS-DNS ($Re_b = 13700, ER = 2$)

A boddy fitted mesh with $332 \times 86 \times 60$ grid points has been used to cover the computational domain. A turbulent and steady channel flow at $Re_\tau = 395$ is used as an inflow, whereas a Neumman condition is applied at the outflow for the velocity and $\tilde{\nu}$ fields. First, the same data and explanation used in

Fig.3 can be applied in this case, though the mesh distribution is slightly different. The benefits of Δ_{lsq} into the mean flow and rms can be appreciated in Fig.6, observing as the shear layer delay is diminished in comparison to $\tilde{\Delta}_{\omega}$. However, both length scales converge with the DNS data downstream of the step edge in the LES part ($x_1 = 4$), regardless of the delay at the shear layer. It would not necessarily be the case in external flows. The unlocking of *KH*instabilities directly impacts the mean flow behaviour, decreasing the flow stiffness at the shear layer and converging to the DNS result. Regarding the

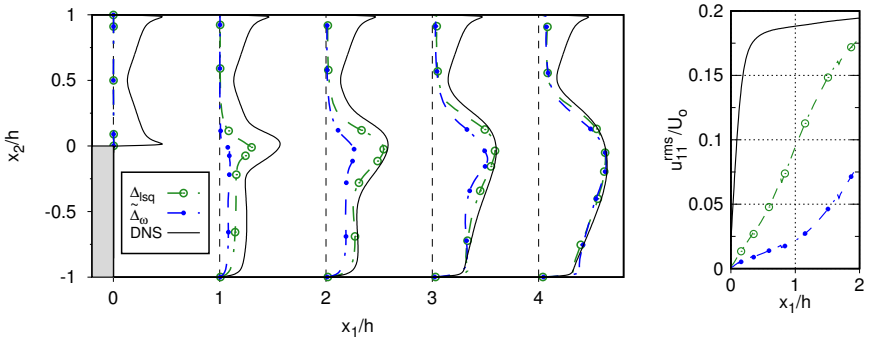

Fig. 6 Resolved Reynolds stresses in the stream-wise direction ($\langle u_{11}^{rms} \rangle$) considering various subgrid length scales (left) and its evolution at $x_2 = 0$ (right). Where U_o refers to the inflow bulk velocity. Reference data, DNS, has been obtained from Pont et al. [3].

$\langle C_f \rangle$ coefficient at the lower wall the improvements triggered by the shear layer are also observed (Fig.7, left, **A**) with Δ_{lsq}. In that case, the $\langle C_f \rangle$ peak is also better captured than the $RANS - SA$ simulation and $\tilde{\Delta}_{\omega}$ (**B**). Moreover, the improvement of $DDES - SA$ respect to the $RANS - SA$ is also evident at the upper wall, where the separation point is delayed (**C**). However, $DDES - SA$ model does not properly capture the channel flow recovering process neither in the upper nor the lower walls (**D**). The $\langle C_f \rangle$ depletion at the upper wall is produced because of the LES interference into the RANS zone, diminishing the eddy viscosity in a place where turbulence is not well triggered yet. Finally, even though acceptable results are obtained with $\tilde{\Delta}_{\omega}$, those are improved with Δ_{lsq} presenting a better transition in the adverse pressure gradient zone. The $RANS - SA$ results are obviously damaged because of its early separation.

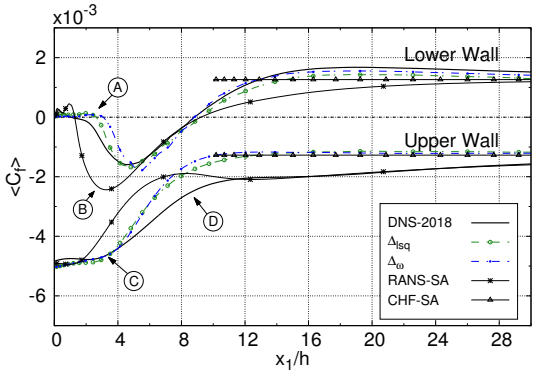

Fig. 7 Skin friction, $\langle C_f \rangle$, at the lower and upper walls downstream of the step edge. Reference data, *DNS*, has been obtained from Pont et al. [3].

6 Conclusions and Future Work

The recent subgrid length scale, Δ_{lsq}, initially developed for LES application by Trias et al. [8], has proved to be a good candidate for *DES* applications. Its good response in shear layer zones with RANS to LES transitions (*GA*), makes that model a natural approach for mitigating the *GA* phenomenon without the need of artificial, and sometimes case dependent, blending functions. However, more challenging flow configurations need to be studied, including computational performance analysis, before considering Δ_{lsq} as a good *GAM* approach.

Acknowledgements

This work has been financially supported by the *Ministerio de Economía y Competitividad*, Spain (No. ENE2017-88697-R). A.P.V. is supported by a *FI-DGR 2016* predoctoral contract (No. 2018FI_B2_00072) financed by *Generalitat de Catalunya*, Spain. F.X.T. is supported by a *Ramón y Cajal* postdoctoral Contract (No. RYC-2012-11996) financed by the *Ministerio de Economía y Competitividad*, Spain.

References

1. Guseva, E.K., Garbaruk, A.V., Strelets, M.K.: Assessment of Delayed DES and Improved Delayed DES Combined with a Shear-Layer-Adapted Subgrid Length-Scale in Separated Flows. Flow, Turbulence and Combustion **98**(2) (2017)
2. Mockett, C., Fuchs, M., Garbaruk, A., Shur, M., Spalart, P., Strelets, M., Thiele, F., Travin, A.: Two Non-zonal Approaches to Accelerate RANS to LES Transition of Free Shear Layers in DES. In: S. Girimaji, W. Haase, S.H. Peng,

D. Schwamborn (eds.) Progress in Hybrid RANS-LES Modelling, pp. 187–201. Springer International Publishing, Cham (2015)
3. Pont-Vílchez, A., Trias, F.X., Gorobets, A., Oliva, A.: Direct Numerical Simulation of Backward-Facing Step flow at $Re_\tau = 395$ and expansion ratio 2. Under Review to the Journal of Fluid Mechanics.
4. Shur, M.L., Spalart, P.R., Strelets, M.K., Travin, A.K.: An Enhanced Version of DES with Rapid Transition from RANS to LES in Separated Flows. Flow, Turbulence and Combustion **95**(4) (2015)
5. Spalart, P., Shur, M., Strelets, M., Travin, A.: Sensitivity of Landing-Gear Noise Predictions by Large-Eddy Simulation to Numerics and Resolution. 50th AIAA Aerospace Sciences Meeting including the New Horizons Forum and Aerospace Exposition (January), 1–20 (2012)
6. Spalart, P.R., Deck, S., Shur, M.L., Squires, K.D., Strelets, M.K., Travin, A.: A new version of detached-eddy simulation, resistant to ambiguous grid densities. Theoretical and Computational Fluid Dynamics **20**(3), 181–195 (2006)
7. Spalart, P.R., Jou, W.H., Strelets, M., Allmaras, S.: Comments on the Feasibility of LES for Wings, and on a Hybrid RANS/LES Approach (1997)
8. Trias, F., Gorobets, A., Oliva, A.: A new subgrid characteristic length for large-eddy simulation. Physics of Fluids **115109** (2017)
9. Vogel, J.C., Eaton, J.K.: Combined Heat Transfer and Fluid Dynamic Measurements Downstream of a Backward-Facing Step **107**(November 1985) (1985)
10. Wray, A.: Unpublished DNS data. Available on AGARD database: "Test Cases for the Validation of Large- Eddy Simulations of Turbulent Flows" (1997). URL ftp://torroja.dmt.upm.es